

## Bulk-mediated surface diffusion along a cylinder: Propagators and crossovers

Aleksei V. Chechkin,<sup>1,2</sup> Irwin M. Zaid,<sup>2</sup> Michael A. Lomholt,<sup>3</sup> Igor M. Sokolov,<sup>4</sup> and Ralf Metzler<sup>2</sup>

<sup>1</sup>*Institute for Theoretical Physics NSC KIPT, Akademicheskaya Street 1, 61108 Kharkov, Ukraine*

<sup>2</sup>*Department of Physics, Technical University of Munich, 85747 Garching, Germany*

<sup>3</sup>*Department of Physics and Chemistry, MEMPHYS-Center for Biomembrane Physics, University of Southern Denmark, Campusvej 55, 5230 Odense M, Denmark*

<sup>4</sup>*Institut für Physik, Humboldt Universität zu Berlin, Newtonstraße 15, 12489 Berlin, Germany*

(Received 20 October 2008; published 27 April 2009)

We consider the effective motion along a cylinder of a particle that freely diffuses in the bulk and intermittently binds to the cylinder. From an exact approach we derive the different regimes of the effective motion along the cylinder characterized by physical rates for binding/unbinding and the bulk diffusivity. We obtain a transient regime of superdiffusion and, interestingly, a saturation regime characteristic for the cylindrical geometry. This saturation in a finite system is not terminal but eventually turns over to normal diffusion along the cylinder. The first passage behavior of particles to the cylinder surface is derived. Consequences for actual systems are discussed.

DOI: 10.1103/PhysRevE.79.040105

PACS number(s): 05.40.Fb, 02.50.Ey, 82.20.-w, 87.16.-b

Bulk-mediated surface diffusion (BMSD) defines the effective surface motion of a particle on a reactive surface that intermittently unbinds and diffuses in the adjacent bulk before rebinding (Fig. 1). BMSD was revealed by NMR in porous glasses [1] and has relevance to numerous technological applications [2]. The particular case of BMSD on a cylindrical surface is of importance for the facilitated diffusion in gene regulation [3,4], the net motion of motor proteins along cytoskeletal filaments [5], the transient binding of chemicals to nanotubes [6], or the exchange behavior between cell surface and surrounding bulk of rod-shaped bacteria (bacilli) and their linear arrangements [7] to name but a few examples.

BMSD was previously investigated for a planar surface in terms of scaling arguments [2,8], master-equation schemes [9], and simulations [10]. More recently the first passage problem between particle unbinding and rebinding for a free cylindrical surface was considered [11]. Here we establish an exact treatment of BMSD for a reactive cylindrical surface deriving explicit expressions for the surface occupation, the effective mean squared displacement (MSD) along the surface, and the returning time distribution from the bulk. Different regimes ranging from transient superdiffusion to terminal normal diffusion emerge naturally from the physical time scales entering our description. We derive previously unknown regimes characteristic of the cylindrical geometry, most remarkably the existence of extremely long jumps as well as a saturation regime of the surface MSD that will be crucial to fully appreciate effective surface motion mediated by bulk diffusion and its experimental investigation.

We consider a cylinder with radius  $a$  centered along the symmetry axis of an outer cylinder of radius  $b$ . As the physically interesting behavior arises along the cylinder, we assume rotational symmetry around the  $z$  axis (Fig. 1). The concentration of particles [density function (DF)] in the bulk is denoted by  $C(r, z, t)$  ( $[C]=\text{cm}^{-3}$ ) while  $n(z, t)$  ( $[n]=\text{cm}^{-1}$ ) refers to the particle DF per length on the inner cylinder surface. The particle numbers are  $N_b(t) = 2\pi \int_a^b r dr \int_{-\infty}^{\infty} C(r, z, t) dz$  in the bulk and  $N_s(t)$

$= \int_{-\infty}^{\infty} n(z, t) dz$  on the cylinder surface. With surface and bulk diffusivities  $D_s$  and  $D_b$  the two densities evolve according to the diffusion equations (a derivation from a discrete model will be presented elsewhere [12])

$$\frac{\partial}{\partial t} n(z, t) = D_s \frac{\partial^2}{\partial z^2} n(z, t) + 2\pi a D_b \left. \frac{\partial C}{\partial r} \right|_{r=a}, \quad (1)$$

in axial direction on the cylinder and

$$\frac{\partial}{\partial t} C(r, z, t) = D_b \left( \frac{1}{r} \frac{\partial}{\partial r} r \frac{\partial}{\partial r} + \frac{\partial^2}{\partial z^2} \right) C(r, z, t), \quad (2)$$

in the bulk using cylindrical coordinates. Note the coupling term between surface and bulk DFs through the flux term in Eq. (1). This term is positive when the particle concentration is higher above the cylinder surface and negative otherwise. We equip the diffusion equations with the following boundary conditions:

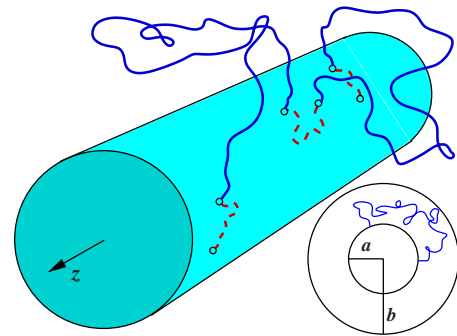


FIG. 1. (Color online) A particle diffuses in the bulk (full lines) and intermittently binds to a cylinder surface on which it may also diffuse (broken lines). This produces an effective surface motion. We here consider the motion along the cylinder. Bottom right: frontal of diffusion between inner and outer cylinders.

$$\lim_{r \rightarrow a} C(r, z, t) = \mu n(z, t), \quad \text{and} \quad \left. \frac{\partial C}{\partial r} \right|_{r=b} = 0. \quad (3)$$

Thus right above the cylinder surface the bulk concentration is defined by the surface density where the coupling constant  $\mu = 1/(2\pi a k_b \tau_{\text{off}})$  involves the binding rate  $k_b$  and the mean unbinding time  $\tau_{\text{off}}$ . The second relation defines a reflecting condition at  $r=b$ . The initial condition corresponds to a sharp concentration at the surface:

$$\lim_{t \rightarrow 0} n(z, t) = N_0 \delta(z) \quad \text{and} \quad \lim_{t \rightarrow 0} C(r, z, t) = 0. \quad (4)$$

Averaging over  $r$  and  $z$  we see that  $N_s(t) + N_b(t) = N_0$ .

Fourier-Laplace transforming the DFs according to

$$C(r, k, u) = \int_{-\infty}^{\infty} dz e^{ikz} \int_0^{\infty} dt e^{-ut} C(r, z, t), \quad (5)$$

and analogously for  $n(k, u)$  (we use the explicit dependence on the Fourier and Laplace variables to denote the transforms), the surface DF yields in the form

$$n(k, u) = \frac{N_0}{u + k^2 D_s + \kappa q \Delta_1 / \Delta}, \quad (6)$$

where  $q = \sqrt{k^2 + u/D_b}$  and  $\kappa \equiv 2\pi a \mu D_b = D_b / (k_b \tau_{\text{off}})$ . We thus find in the denominator of the usual diffusion propagator a correction proportional to  $\kappa$  stemming from the bulk exchange. For the bulk DF we obtain

$$C(r, k, u) = \mu N_0 \frac{K_1(qb)I_0(qr) + I_1(qb)K_0(qr)}{\Delta[u + D_s k^2 + \kappa q \Delta_1 / \Delta]}, \quad (7)$$

where the  $\Delta$  factors are defined as follows:

$$\begin{aligned} \Delta_1 &= K_1(qa)I_1(qb) - I_1(qa)K_1(qb), \\ \Delta &= I_0(qa)K_1(qb) + I_1(qb)K_0(qa), \end{aligned} \quad (8)$$

in terms of the modified Bessel functions.

We note that the coupling strength  $\kappa$  is a measure for the efficiency of the bulk-surface exchange. At  $\kappa=0$  the number of surface particles  $N_s(t)$  remains constant. We define the coupling time scale

$$t_\kappa = D_b / \kappa^2 = [k_b \tau_{\text{off}}]^2 / D_b, \quad (9)$$

which tends to infinity for vanishing coupling and to zero for strong coupling ( $\kappa \rightarrow \infty$ ). From the diffusion behavior we extract two additional time scales, namely,

$$t_a = a^2 / D_b \quad \text{and} \quad t_b = b^2 / D_b. \quad (10)$$

For times shorter than  $t_a$  the particle does not yet sense the curvature of the cylinder surface while for times longer than  $t_b$  it feels the confinement by the outer cylinder. In what follows we are mainly interested in the regime of strong coupling  $t_\kappa \ll t_a \ll t_b$  but will also report an almost ballistic behavior under weaker coupling. The remaining cases will be discussed elsewhere [12].

The number of adsorbed particles follows from  $n(k, u)$  by taking  $k \rightarrow 0$ . For short times  $t \ll t_\kappa$  we find that  $N_s(t) \approx N_0$  remains constant as it should by definition of the coupling

time. At longer times  $t_\kappa \ll t \ll t_a$  the behavior changes to  $N_s(t) \approx N_0 \sqrt{t_\kappa / [\pi t]} \approx t^{-1/2}$ . For even longer times  $t_a \ll t \ll t_b$  we have a faster decay  $N_s(t) \approx \frac{1}{2} N_0 \sqrt{t_\kappa t_a / t}$  inversely proportional to  $t$ . Finally at very long times  $t \gg t_b$  the dynamics equilibrates with respect to the radial diffusion and  $N_s(t) \approx 2N_0 \sqrt{t_\kappa t_a / t_b}$ .

*Axial diffusion.* The MSD along the cylinder surface can be obtained from the characteristic function through

$$\langle z^2(u) \rangle = -N_0^{-1} \left. \frac{\partial^2 n(k, u)}{\partial k^2} \right|_{k=0}, \quad (11)$$

where we divide by  $N_0$  to obtain an effective one-particle displacement. This quantity is not corrected for particles leaving the surface in contrast to the normalized displacement  $\langle z^2(u) \rangle_n = N_0 \langle z^2(u) \rangle / N_s(t)$ . For the MSD along the cylinder we find at short times ( $t \ll t_\kappa$ ),

$$\langle z^2(t) \rangle \sim 2D_s t \left[ 1 + \frac{2}{3\sqrt{\pi}} \frac{D_b}{D_s} \left( \frac{t}{t_\kappa} \right)^{1/2} \right] \sim \langle z^2(t) \rangle_n. \quad (12)$$

Thus, in this regime the diffusion to leading order is confined to the surface; exchange with the bulk leads to a higher order superdiffusive correction, when  $D_s \ll D_b$  (see below). Conversely, for longer times  $t_\kappa \ll t \ll t_a$ ,  $N_s(t)$  decays perceptibly and

$$\langle z^2(t) \rangle \sim 2D_s t_\kappa + \frac{2}{\sqrt{\pi}} D_b \sqrt{t t_\kappa}, \quad (13a)$$

$$\langle z^2(t) \rangle_n \sim 2\sqrt{\pi} D_s \sqrt{t t_\kappa} + 2D_b t. \quad (13b)$$

At even longer times  $t_a \ll t \ll t_b$  we see the influence of the cylindrical geometry in the logarithmic dependencies

$$\langle z^2(t) \rangle \sim \frac{D_s t_a t_\kappa}{t} \log \left( \frac{4t}{C t_a} \right) + D_b \sqrt{t_a t_\kappa}, \quad (14a)$$

$$\langle z^2(t) \rangle_n \sim 2D_s \sqrt{t_a t_\kappa} \log \left( \frac{4t}{C t_a} \right) + 2D_b t, \quad (14b)$$

with Euler's constant  $\log C = \gamma = 0.5772$ .  $\langle z^2(t) \rangle$  exhibits a saturation unique to the cylinder case due to the fast decay of surface particles,  $N_s(t) \approx 1/t$ , see above. Finally, at very long times  $t \gg t_b$  due to radial equilibration a linear diffusive behavior yields

$$\langle z^2(t) \rangle \sim \frac{8t_a t_\kappa}{t_b^2} D_s t + 4D_b \frac{\sqrt{t_a t_\kappa}}{t_b}, \quad (15a)$$

$$\langle z^2(t) \rangle_n \sim 4D_s \frac{\sqrt{t_a t_\kappa}}{t_b} + 2D_b t, \quad (15b)$$

i.e., the combination of diffusion in the bulk and along the cylinder gives rise to an effective diffusivity involving all time scales.

The behavior of the MSD  $\langle z^2(t) \rangle$  for  $D_s=0$  is shown in Fig. 2. Note that the time scales (in dimensionless units)  $t_\kappa = 10^{-6}$ ,  $t_a = 1$ , and  $t_b = 10^6$  were chosen to be well separated

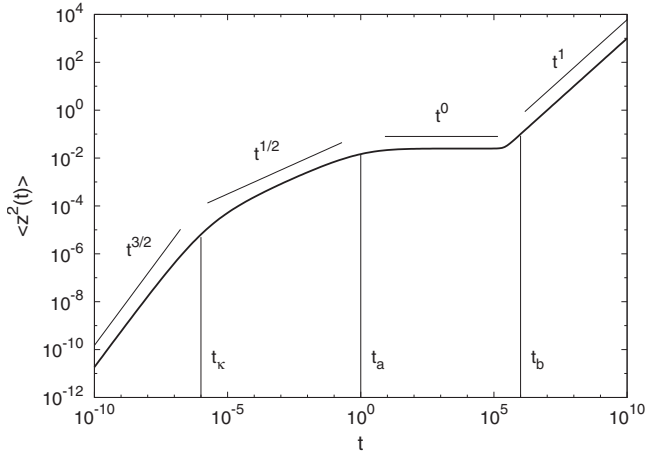


FIG. 2. MSD obtained from numerical Laplace inversion of Eqs. (6), (8), and (11), showing the various effective diffusion regimes along the cylinder. Note the transient plateau.

to visualize the four scaling regimes. The other parameters were  $a=5$ ,  $D_b=a^2/t_a=25$ ,  $\kappa=a/\sqrt{t_a t_\kappa}=5 \times 10^3$ , and  $b=a\sqrt{t_b/t_a}=5 \times 10^3$ .

*Propagator:* Our formalism also produces the exact distributions  $C(r,t)$  and  $n(z,t)$ . For times longer than  $t_b$  we already found that the diffusion behavior is normal albeit with rescaled diffusivity and the propagator along the cylinder turns into a Gaussian. We recover a Gaussian for  $n(z,t)$  in absence of bulk coupling,  $\kappa=0$ . For times shorter than  $t_b$  and  $\kappa>0$  we observe non-Gaussian behavior. In most relevant cases  $D_s \ll D_b$  and we therefore consider the case  $D_s=0$  in what follows.

At shorter times  $t \ll t_a < t_b$  we have  $ut_a \gg 1$  and  $ut_b \gg 1$ , and  $qa = a\sqrt{k^2 + u/D_b} \geq a\sqrt{u/D_b} = \sqrt{ut_a} \gg 1$  such that  $qa \gg 1$  and  $qb \gg 1$ . Therefore  $\Delta_1 \approx \Delta$  and the propagator reduces to

$$n(k,u) = \frac{N_0}{u + \kappa\sqrt{k^2 + u/D_b}}. \quad (16)$$

In the central part of the DF where  $k^2 > u/D_b$  (i.e.,  $z < \sqrt{D_b t}$ ), we obtain the normalized Cauchy distribution

$$n(k,u) = \frac{N_0}{u + \kappa|k|} \Leftrightarrow n(z,t) = \frac{N_0 \kappa t}{\pi(z^2 + \kappa^2 t^2)}. \quad (17)$$

This interesting result is analogous to the findings from Ref. [2] for a flat surface found from scaling arguments [13]. Here we derive the Cauchy law from an exact approach allowing us to study the transition to other regimes explicitly. To do so we introduce the range of validity  $\ell_c(t) = \sqrt{D_b t}$  of the Cauchy region. While at distances  $z > \ell_c(t)$  we observe a Gaussian cutoff, for  $z < \ell_c(t)$  the Cauchy approximation is valid. From this Cauchy part we obtain the superdiffusive contribution,

$$\int_{-\ell_c(t)}^{\ell_c(t)} \frac{z^2 \kappa t dz}{\pi(z^2 + \kappa^2 t^2)} \sim 2\kappa\sqrt{D_b} t^{3/2}, \quad (18)$$

to the MSD, consistent with exact result (12) (with  $D_s=0$ ). Calculation of the MSD from full Eq. (6) however requires the  $k \rightarrow 0$  limit and thus the extreme wings of the distribution are explored. As the system evolves in time the central

Cauchy part spreads. As in the regime  $t_\kappa < t < t_a$  we already have  $D_b t < \kappa^2 t^2$ , the asymptotic behavior  $\approx z^{-2}$  can no longer be observed.

At intermediate times  $t_\kappa \ll t \ll t_a$  we find  $n(k,u) = N_0 \sqrt{t_\kappa} / (u + D_b k^2)$  corresponding to the Gaussian

$$n(z,t) = N_s(t) \sqrt{\frac{1}{4\pi D_b t}} \exp\left(-\frac{z^2}{4D_b t}\right), \quad (19)$$

with  $N_s(t) = \int_{-\infty}^{\infty} n(z,t) dz = N_0 \sqrt{t_\kappa} / (\pi t)$ . For longer times  $t_a \ll t \ll t_b$  the propagator acquires the shape  $n(k,u) = -a N_0 \log(C^2 [a^2 k^2 + ut_a] / 4) / [2\kappa]$  which yields Eq. (19) with  $N_s(t) = N_0 \sqrt{t_a t_\kappa} / [2t]$ . Finally, for very long times  $t \gg t_b$  we again find Eq. (19) with the saturation value  $N_s(t) = 2N_0 \sqrt{t_a t_\kappa} / t_b$ . Indeed one can show by the shift theorem of the Laplace transformation that any function of the argument  $u + D_b k^2$  will lead to Gaussian shape (19), with appropriate normalization.

*First passage.* The DF of times  $\varphi(t)$  a particle spends in the bulk after detachment from the cylinder can be calculated explicitly (details of the calculation will be presented elsewhere [12]). To this end we initially place the test particle at radius  $a < r_0 < b$  and calculate when it is first adsorbed at  $r=a$ . With  $t_0 = r_0^2 / D_b$  this first passage problem defines  $\varphi(t)$  by

$$\varphi(t) = 2\pi a \int_{-\infty}^{\infty} D_b \left. \frac{\partial C(r,z,t)}{\partial r} \right|_{r=a} dz, \quad (20)$$

in terms of the radial flux into  $r=a$ . The Laplace transform of  $\varphi(t)$  then becomes

$$\varphi(u) = \frac{I_1(\sqrt{ut_b})K_0(\sqrt{ut_0}) + K_1(\sqrt{ut_b})I_0(\sqrt{ut_0})}{I_1(\sqrt{ut_b})K_0(\sqrt{ut_a}) + K_1(\sqrt{ut_b})I_0(\sqrt{ut_a})}. \quad (21)$$

For  $t_b \rightarrow \infty$ ,  $\varphi(u) \sim K_0(\sqrt{ut_0}) / K_0(\sqrt{ut_a})$  while for  $r_0 = a$  we recover the sharp form  $\varphi(t) = \delta(t)$  as it should.

At shorter times  $t \ll t_a < t_0$  we obtain the expansion

$$\varphi(t) = \sqrt{\frac{a}{r_0}} \frac{r_0 - a}{\sqrt{4\pi D_b t^3}} e^{-(r_0 - a)^2 / 4D_b t} \left(1 + \frac{D_b t}{4ar_0} + \dots\right). \quad (22)$$

This expression, to leading order, corresponds to the first passage DF of a one-dimensional (1D) random walk, reweighted by the ratio  $\sqrt{a}/r_0$ . Keeping the distance  $r_0 - a$  fixed but letting both  $r_0$  and  $a$  tend to infinity, we recover the result for a flat surface for which the 1D first passage remains valid at all times.

At longer times  $t_a \ll t \ll t_b$  the logarithmic form  $\varphi(u) \sim 1 - 2 \log(r_0/a) / \log(1/[ut_a])$  yields. From Tauberian theorems [14] we infer the first passage behavior into a cylinder of radius  $a$ ,

$$\varphi(t) \sim \frac{2 \log(r_0/a)}{t \log^2(t/t_a)}, \quad (23)$$

see also Refs. [11,15]. We note that a distribution of return times to the cylinder of this form implies by a diffusive coupling  $z^2 \approx t$  that a single bulk excursion leads to the DF  $\lambda(z) \approx 1/(z \log^2 z)$  of effective dislocations  $z$  along the cyl-

inder. Finally in the long-time limit  $t \gg t_b$  the outer cylinder comes into play and  $\varphi(t)$  attains an exponential cutoff, leading to a mean first passage time

$$\langle t \rangle = b^2 \log(r_0/a)/[2D_b]. \quad (24)$$

*Extremely long jumps.* An interesting behavior occurs when we relax the strong-coupling condition  $t_\kappa \ll t_a$ . We said that when  $t \gg t_a$  the diffusing particles feel a change in geometry from planar to cylindrical, and the time scale  $t_c \equiv \sqrt{t_a t_\kappa} = a/\kappa$  occurs in our expressions. If we have  $t_a \ll t \ll t_c \ll t_b$  then  $N_s(t) \approx N_0$  and

$$\langle z^2(t) \rangle = 2D_s t + \frac{2D_b t^2}{t_c \log^2[4t/(C^2 t_a)]}, \quad (25)$$

which is a ballistic behavior with logarithmic correction: for  $D_s \ll D_b$  the superdiffusion is even stronger than for  $t \ll t_a$ . Similarly, the propagator reduces to

$$n(k, u) = N_0/[u + \kappa q K_1(aq)/K_0(aq)]. \quad (26)$$

In the range  $a \ll z \ll \sqrt{D_b t}$  (i.e.,  $\sqrt{u t_a} \ll a k \ll 1$ ),  $\kappa q K_1(aq)/K_0(aq) \sim (\kappa/a) \log[2/(Cak)]$ , which is an extremely weak  $k$  dependence: this precutoff tail of  $n(k, u)$  is heavier than any normalizable power law due to the heavy tailed distribution of bulk mediated dislocations.

*Discussion.* We established an exact approach to BMSD along a reactive cylindrical surface revealing four distinct diffusion regimes. In particular our formalism provides a stringent derivation of the transient superdiffusion discussed earlier and explicitly quantifies the transition to other regimes. Notably we revealed a saturation regime for the MSD along the cylinder that becomes relevant at times above which the diffusing particle feels the curvature of the cylinder surface ( $t_a$ ). This behavior, caused by the cylindrical geometry, stems from an interesting balance between a net flux

of particles into the bulk and the fact that particles with a longer return time also lead to an increased effective surface relocation. In absence of an outer cylinder the saturation is terminal while in its presence the MSD along the cylinder returns to a linear growth in time. This observation will be important in future models of BMSD around cylinders and particularly for the interpretation of experimental data obtained for BMSD systems. We note that in the proper limit  $a \rightarrow \infty$  the previous results for a planar surface are recovered. Relaxing the strong-coupling condition we demonstrated the existence of an almost ballistic BMSD behavior, a case that might be relevant for transport along thin cylinders such as DNA.

In Ref. [11] it was shown that the scaling behavior in the regimes below and above  $t_a$  can be probed experimentally by NMR methods measuring the BMSD of water molecules along imogolite nanorods over three orders of magnitude in frequency space. For larger molecules such as a protein of approximate diameter of 5 nm, we observe a diffusivity of  $10^{-6}$  cm<sup>2</sup>/s such that for instance the saturation plateau around a bacillus cell (radius 1/2  $\mu$ m) sets in at around  $t_a = 2.5$  ms which might give rise to interesting consequences for the material exchange around such cells. In general, the relevance of the individual regimes will crucially depend on the scales of the surface radius and the diffusing particle (and therefore its diffusivity). It was discussed previously that even the superdiffusive short-term behavior may become relevant [2,8,10]. In general, in a given system the separation between the various scaling regimes may not be sharp. Moreover typically a single experimental technique will not be able to probe all regimes. It is therefore vital to have available a solution for the entire BMSD problem.

Support from DFG and the EC (Grant No. MC-III-F 219966) are acknowledged.

- 
- [1] S. Stapf, R. Kimmich, and R.-O. Seitter, *Phys. Rev. Lett.* **75**, 2855 (1995).  
 [2] O. V. Bychuk and B. O'Shaughnessy, *J. Chem. Phys.* **101**, 772 (1994).  
 [3] P. H. von Hippel and O. G. Berg, *J. Biol. Chem.* **264**, 675 (1989).  
 [4] M. A. Lomholt, T. Ambjörnsson, and R. Metzler, *Phys. Rev. Lett.* **95**, 260603 (2005).  
 [5] C. Bustamante, Y. R. Chemla, N. R. Forde, and D. Izhaky, *Annu. Rev. Biochem.* **73**, 705 (2004).  
 [6] M. V. Veloso, A. G. Souza Filho, J. Mendes Filho, Solange B. Fagan, and R. Mota, *Chem. Phys. Lett.* **430**, 71 (2006).  
 [7] S. I. Coyne and N. H. Mendelson, *Infect. Immun.* **12**, 1189 (1975).  
 [8] O. V. Bychuk and B. O'Shaughnessy, *Phys. Rev. Lett.* **74**, 1795 (1995).  
 [9] J. A. Revelli, C. E. Budde, D. Prato, and H. S. Wio, *New J. Phys.* **7**, 16 (2005).  
 [10] R. Valiullin, R. Kimmich, and N. Fatkullin, *Phys. Rev. E* **56**, 4371 (1997).  
 [11] P. Levitz, M. Zinsmeister, P. Davidson, D. Constantin, and O. Poncelet, *Phys. Rev. E* **78**, 030102(R) (2008).  
 [12] A. V. Chechkin, I. M. Zaid, I. M. Sokolov, M. A. Lomholt, and R. Metzler, (unpublished).  
 [13] Substituting  $x^2 + z^2$  for  $r^2$  in Eq. (6) of Ref. [2] and integrating  $x$  over  $(-\infty, \infty)$  produces Eq. (17).  
 [14] S. Havlin and G. H. Weiss, *J. Stat. Phys.* **58**, 1267 (1990).  
 [15] S. Redner, *A Guide to First-Passage Processes* (Cambridge University Press, Cambridge, 2001).